

# LONG-TERM CORRELATIONS IN SHORT, NON-STATIONARY TIME SERIES: AN APPLICATION TO INTERNATIONAL R&D COLLABORATIONS

Lorenzo Righetto\*    Alessandro Spelta<sup>†</sup>    Emanuele Rabosio<sup>‡</sup>  
Fabio Pammolli<sup>§¶</sup>

February 18, 2019

## Abstract

Within the perimeter of patent collaboration networks, the average distance of collaborations and the number of countries involved per each collaboration have been shown to have increased steadily in time. Less attention, though, has been devoted to assessing whether growth of cross-country collaborations is stable or robust in time. To address this scientific question we focus on the identification of long-term correlations (i.e. persistence in time). Our data sets consists of time series of yearly average collaboration radii and of cross-border links in the Euro-American subsystem of the global collaboration network for the period 1978 - 2014. To detect long-term correlations, we use Detrended Fluctuation Analysis, a method that is used to measure persistence in signals. In addition, we devise a general and original procedure to assess the statistical significance of results for short time series. Our results, showing that long-term correlations do exist in the great majority of our signals, reinforce the hypothesis of a diminishing role of geographical distance in technological collaborations. Results at the level of nations show that a significant degree of heterogeneity in scaling values can be detected within Europe, irrespectively of the substantial efforts towards the set-up of an integrated European Research Area.

R&D international collaborations Detrended Fluctuation Analysis integration of R&D systems

---

\*Center for Analysis, Decisions, and Society (CADS) - Human Technopole, Milano, Italy; lorenzo.righetto@htechnopole.it

<sup>†</sup>Center for Analysis, Decisions, and Society (CADS) - Human Technopole, Milano, Italy; alessandro.spelta@htechnopole.it

<sup>‡</sup>Center for Analysis, Decisions, and Society (CADS) - Human Technopole, Milano, Italy; emanuele.rabosio@htechnopole.it

<sup>§</sup>Politecnico di Milano, Department of Management, Economics and Industrial Engineering; fabio.pammolli@polimi.it

<sup>¶</sup>Center for Analysis, Decisions, and Society (CADS) - Human Technopole, Milano, Italy

# 1 Introduction

2 Networks of collaborative agreements are recognized as an ever-widening organization  
3 form, especially in high technology, knowledge-intensive fields (Arora and Gambardella,  
4 1994; Arora et al., 2001; Orsenigo et al., 2001). In particular, networks of collabora-  
5 tions among innovators have been indeed extensively used to represent and analyze the  
6 division of innovative labor since the seminal paper by Freeman (Freeman, 1991). The  
7 structure of the international network of patent collaboration, in terms of co-inventions or  
8 co-assignment of patents, has been evaluated broadly in recent literature and the average  
9 distance of collaborations, together with the number of countries involved per each collabora-  
10 tion, has been shown to have increased steadily in time (Chessa et al., 2013; Morescalchi  
11 et al., 2015). Several factors play a role in this ongoing phenomenon, including increasing  
12 ease of knowledge sharing, physical transportation, diminishing language barriers, and  
13 so on. Similar studies concerning academic research collaborations have shown gener-  
14 ally coherent results (Frenken et al.; Hoekman et al., 2010; Waltman et al., 2011), with  
15 some notable exceptions highlighting the concurrent domestic increase of collaborations  
16 (Maisonobe et al., 2016). Despite the growing body of literature on knowledge networks,  
17 the analysis of their temporal evolution still remains at its infancy. Less attention has  
18 been indeed devoted, for instance, to assessing whether the growth of geographical dis-  
19 tance and of the number of cross-country technological collaborations may be considered  
20 stable or robust, beyond the common global trend associated with the globalization. In  
21 this paper, we make use of Detrended Fluctuation Analysis (DFA) (Peng et al., 1994)  
22 to detect the presence of long-term correlations in our time series. In other words, this  
23 corresponds to determining whether the observed increases in geopolitical features of tech-  
24 nological collaborations can be considered persistent in time. So far, DFA has been used  
25 in different fields, e.g. to investigate diseased states in physiological studies (Hardstone  
26 et al., 2012), as well as prey search behaviors in ecological studies (Viswanathan et al.,  
27 1996).

28 In the context of R&D collaborations, this analysis can be used to bring further evi-  
29 dence of a decreasing role of distance, in the context of globalization (Disdier and Head,  
30 2008), in case collaboration patterns are shown to display such long-term correlations –  
31 e.g. meaning that the increase of the distances of collaborations in the short run makes  
32 them more likely to increase also in the future. In fact, DFA represents a useful tool as  
33 it purges the signal from the underlying trends and is, as such, particularly indicated for  
34 time series which exhibit strong non-stationarity (Hu et al., 2001), as we observe in this  
35 case (see Chessa et al., 2013; Morescalchi et al., 2015). We apply DFA to time series of  
36 yearly average collaboration radii and of yearly number of cross-border links, recorded for  
37 all collaborations (co-inventions and co-assignments) at the OECD TL3 aggregation scale  
38 – all regions in the European Union (EU) and in the United States (US) are considered  
39 – from OECD RegPat registry of patent applications, which currently spans from 1978  
40 to 2014. We choose to track both these measures, even though they convey similar infor-  
41 mation, for several reasons - for instance, to control for specific geographical, historical  
42 or economic reasons that might make it easier for a region to initiate international col-  
43 laborations, but in a limited geographical range. We restrict the analysis to the EU+US  
44 subsystem to better highlight the role of US nodes in determining the observed EU scal-  
45 ing values, in line with previous literature focusing on these two important subsystems

46 (Owen-Smith et al., 2002; Chessa et al., 2013). We aggregate results at the national level  
47 (and, for the most part, at “continental” level) as in Viswanathan et al. (1996) to obtain  
48 a more reliable estimate of scaling behaviours.

49 In the literature, several papers have highlighted the shortcomings of the DFA method  
50 in terms of estimation errors for short time series (see e.g. Delignieres et al., 2006) or even  
51 of its real detrending power (Bryce and Sprague, 2012). We take into account these fore-  
52 warnings by performing several controls on synthetically generated time series of specified  
53 length and known DFA scaling. On one side, we make sure that trend removal is actually  
54 performed, following Hu et al. (2001). On the other side, by repeating the synthetic gen-  
55 eration of time series, we obtain a measure of the estimation error at varying time series  
56 length and scaling factor. We use these measures to complement our empirical observa-  
57 tions with confidence intervals, e.g. to detect whether uncorrelation can be excluded with  
58 statistical significance.

59 Results show that long-term correlations do exist in the great majority of our signals.  
60 This result shows that the suppression of the global underlying trend does not affect the  
61 positive long-term correlation of the selected time series. This general result does not  
62 prevent us from running comparisons, e.g. between the EU+US system and each possible  
63 subsystem – down to European national level – to detect marginal effects of, say, including  
64 US nodes to the magnitude of long-term positive correlations in EU signals. In particular,  
65 we assess the degree of heterogeneity of observed scaling values among EU countries, to  
66 evaluate the deviation of the system from a completely integrated European R&D area.

67 The paper is organized as follows. Section 2 describes the dataset we use and the  
68 metrics we extract from it. We describe in Section 3 the DFA method in general and  
69 in the specific application to our case study. Section 4 is devoted to the presentation of  
70 results and their discussion. Conclusions in Section 5 close the paper. In the Appendix,  
71 we describe the details of our DFA application to the case under study and the controls  
72 on the soundness of our DFA scaling value estimation.

## 73 2 Data

74 We make use of the data provided by the OECD RegPat registry, which contains all  
75 patent records from the European Patent Office (EPO) since the first application (1978)  
76 until present. We treat 2014 as the latest complete year of application to allow for the  
77 review process to be completed for all patents in that year. In addition to that, in RegPat  
78 all assignee and inventor addresses are attributed a single OECD TL3 level geographical  
79 location for each of the OECD partner countries. We restrict our analysis to EU and  
80 US regions, which constitute, together, around 85% of the total number of OECD TL3  
81 regions in RegPat (4700 out of 5552). This spatial segmentation corresponds to NUTS3  
82 regions for EU and to counties for US. We complement this dataset by calculating centroid  
83 coordinates for each of these regions. To increase the number of nodes in this network,  
84 we use all European regions within the 2013 edition of the NUTS3 map (which also  
85 includes not “full” EU countries such as Switzerland and Turkey). What we obtain  
86 is a spatial characterization of the patent collaboration network, which we analyze in  
87 terms of co-assignments (companies collaborating for R&D regarding a specific patent)  
88 and co-inventions (different scientists/researchers collaborating as part of one or more  
89 organizations). In the former case, the reported address is related to the location of the

90 company’s headquarter, while in the latter case the location may refer to the inventor’s  
 91 residence or the address of her/his working place (which may differ from the related  
 92 assignee’s headquarter address, of course).

93 We extract all patent numbers which relate to multiple records (i.e. the patent is  
 94 the result of a co-assignment or of a co-invention) and compute two metrics from each  
 95 collaboration and for each of the involved nodes (regions):

- 96 • the average of the distance (which we call *radius of co-assignment/co-invention*,  
 97  $\rho_A/\rho_I$  in symbols) from the focal node to all other collaborating nodes (this metric  
 98 can be zero), computed on a sphere and expressed in kilometres;
- 99 • the number of cross-border (i.e. cross-country or cross-state in the US case) links  
 100 that the focal node collects within the collaboration (again, this metric can be zero).  
 101 Cross-border links for co-assignments and co-inventions are expressed as  $CB_A/CB_I$   
 102 in symbols, respectively.

103 We aggregate these metrics by computing the average yearly radius of collaboration  
 104 (no finer temporal scale is allowed by the RegPat database) and the yearly sum of cross-  
 105 border links in each node. We repeat this calculation for 3 different segmentations of our  
 106 network:

- 107 • EU: only European nodes are considered (i.e. US nodes do not contribute to the  
 108 computations);
- 109 • US: only US nodes are considered (cross-border links, in this case, refer to *cross-state*  
 110 links);
- 111 • EU+US: the whole system is considered.

112 In the end, we obtain time series of both metrics for all nodes covered by the focal  
 113 segmentation and for the time span 1978-2014. We further exclude the starting year 1978  
 114 since the number of applications was extremely low, around 0.1% of the total.

### 115 3 Detrended Fluctuation Analysis

116 We make use of DFA (Peng et al., 1994), a widely used technique for the identification  
 117 of long-term correlations in time series (see e.g. Hardstone et al. (2012) for a compelling  
 118 review of this method). The first step of DFA consists in transforming the time series  
 119 under study in a random walk path, by integrating the time series  $x(t)$  as follows:

$$y(t) = \sum_{k=1}^t [x(k) - \langle x \rangle], \quad (1)$$

120 where  $\langle x \rangle$  is the mean value of  $x(t)$ . The transformed signal is then segmented  
 121 in windows of various sizes  $\Delta n$ . In each window, and repeatedly for all values of  $\Delta n$ , a  
 122 polynomial of order  $s$  (hence, the order of the DFA applied to the focal case is fitted to  
 123 the integrated data, in order to obtain an estimated set of points  $y'(k)$ . Please note that,  
 124 as a result of the controls we perform (see the Appendix), we choose to use DFA-2 (i.e.  
 125  $s = 2$ ). The value of the *fluctuation function*  $F(\Delta n)$  for that particular value of  $\Delta n$  is

126 the average of the standard deviation between the polynomial fit  $y'$  and the data, over all  
 127 data points  $N$ , for all windows:

$$F(\Delta n) = \sqrt{\frac{1}{N} \sum_{k=1}^N [y'(k) - y(k)]^2} \quad (2)$$

128 When  $F(\Delta n)$  is plotted against  $\Delta n$  in a double-logarithmic plot, the relationship is  
 129 expected to be linear and the slope of the regression line defines the DFA scaling  $\alpha$ .  
 130 This scaling is a measure of the presence of self-similarity and, relatedly, of long-term  
 131 correlations in the signal, as it tracks down the scaling of dispersion around a regressor  
 132 for increasing window sizes. In particular, the value of  $\alpha$  can describe the following signal  
 133 behaviours:

- 134 •  $0 < \alpha < 0.5$ : the signal has long-term memory and is anti-correlated;
- 135 •  $0.5 < \alpha < 1$ : the signal has long-term memory and is correlated;
- 136 •  $\alpha = 0.5$ : the signal is uncorrelated (has no memory);
- 137 •  $\alpha > 1$ : the signal is non-stationary.

138 This relates to the intrinsic properties of the signal in the sense that, at least in  
 139 the range between 0 and 1, it represents three different behaviors of the random walker  
 140 corresponding to the time series under study (see also Fig. 3 in [Hardstone et al., 2012](#),  
 141 for a pictorial representation) :

- 142 •  $0 < \alpha < 0.5$  (anti-correlation): the random walker moves preferentially in the  
 143 opposite direction with respect to the previous step; the resulting cumulated walk  
 144 (i.e. cumulated time series) will show very small fluctuations in time and thus the  
 145 slope of the fluctuation function at increasing window sizes will be relatively low;
- 146 •  $0.5 < \alpha < 1$  (correlation): the random walker tends to repeat the same moves it  
 147 has performed previously, inducing wide fluctuations in time; thus, when measuring  
 148 the error between a regressor and the data at large window sizes, this error will be  
 149 much larger than the error measured at small window sizes (i.e. a higher slope);
- 150 •  $\alpha = 0.5$ : when the choice of a direction of movement is independent from the  
 151 previous steps, in analogy with pure diffusion the mean square displacement in time  
 152 of the random walker will scale as 0.5.

153 In our case study, following [Viswanathan et al. \(1996\)](#), we extend the method to the  
 154 case of several short signals grouped together, by calculating  $F(\Delta n)$  over all possible  
 155 windows in the subsystem under study. In brief, each value of the standard deviation  
 156 of residuals is averaged over  $N$  (the size of the individual time series, i.e. 36) times  
 157 the number of nodes constituting that particular subsystem. We use here 6 values of  
 158  $\Delta n$ , corresponding to the exact divisors of 36 (i.e.  $\Delta n = 4, 6, 9, 12, 18, 36$ ). We also  
 159 standardize values with respect to individual mean and standard deviation values, to  
 160 further homogenize the sample data in terms of geographical range and country “size”.

Subsystem	$\rho_A$	$\rho_I$	$CB_A$	$CB_I$
EU	0.37	0.30	0.22	0.75
US	0.15	0.12	0.20	0.37
EU+US	0.28	0.19	0.23	0.52
$(EU+US)_{EU}$	0.40	0.31	0.26	0.78
$(EU+US)_{US}$	0.17	0.13	0.18	0.30

**Table 1:** Fraction of nodes in each subsystem displaying a monotonic trend according to Mann-Kendall test.  $\rho_A$ : average yearly radius of co-assignment;  $\rho_I$ : average yearly radius of co-invention;  $CB_A$ : number of yearly cross-border links according to co-assignments;  $CB_I$ : number of yearly cross-border links according to co-inventions.

161 We are aware, of course, that the series under study might contain strong non-  
162 stationarities which might undermine the results of DFA (Bryce and Sprague, 2012). Nev-  
163 ertheless, the effect of trends on DFA has been studied in the literature and workarounds  
164 to ascertain the true underlying scaling of the signal have been demonstrated in Hu et al.  
165 (2001). In particular, in Hu et al. (2001) it emerges that DFA of order  $x$  (termed DFA- $x$ )  
166 can only neutralize the effect of  $x - 1$  order trends. For additional information on the  
167 application of DFA to our case study and on the controls we performed (including the  
168 ones for determining the actual detrending power of DFA in our case), please see the  
169 Appendix.

## 170 4 Results and Discussion

171 As a first assessment of the general evolution of the metrics under study, we calculate  
172 the prevalence of nodes for which a Mann-Kendall test at significance level 0.05 detects a  
173 monotonic trend. We report the results in Table 1. The values we obtain are substantial,  
174 confirming that there is an underlying global trend in this metrics that is affecting a  
175 large portion of regions, especially in the EU. As a caveat, we have to specify that higher  
176 statistics we obtain for the EU system, with respect to the US system, are likely to be  
177 due to the “submission bias” that is intrinsic to using the RegPat database (which comes  
178 from EPO data). In this respect, results concerning the US subsystem should be looked  
179 at in relative terms.

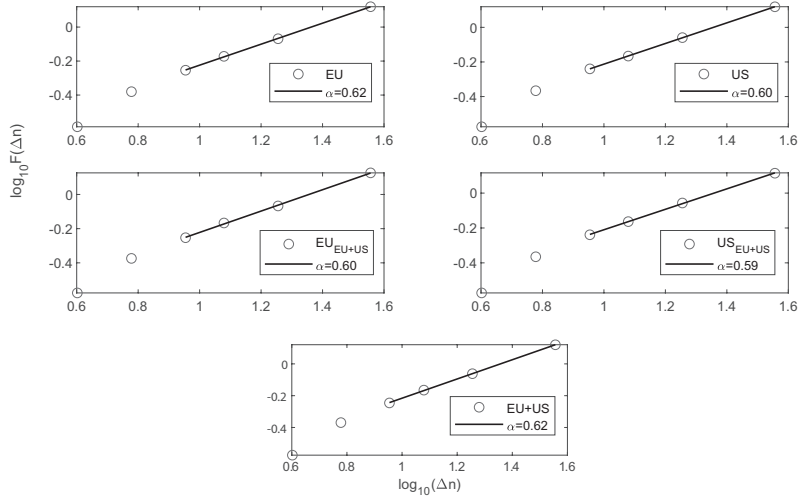
180 Despite the high prevalence of non-stationary individual signals in our data, our ap-  
181 plication of DFA-2 can purge the trend effects from the estimated scaling, as shown in  
182 the Appendix. Table 2 shows the results of the application of the method to the 3 se-  
183 lected subsystems, plus the scaling obtained when the EU and the US are embedded in  
184 the EU+US system. This allows us to detect positive or negative effects of a combined  
185 collaboration system on the robustness of these series. In very general terms, scaling  
186 values turn out to indicate positive long-term correlation in all the selected subsystems,  
187 for all metrics analyzed (see Fig. 1 for an example of fluctuation plots and their relative  
188 estimated scaling). We confirm this result by reshuffling our data series, as performed in  
189 Castillo et al. (2015). We randomly reassign data points to different nodes for each year  
190 and estimate the DFA-2 scaling. We verify that series become uncorrelated in this case  
191 (i.e. values lie within the 5-95<sup>th</sup> percentile region of an uncorrelated synthetic signal).

192 Co-assignment metrics also show lower scaling values than those regarding co-invention  
193 metrics, as a result of co-assignment being a much rarer occurrence. As specified earlier,  
194 US scaling values are generally lower than in the EU subsystem, except for that of the

Subsystem	$\rho_A$	$\rho_I$	$CB_A$	$CB_I$
EU	0.62	0.68	0.62	0.69
US	0.60	0.71	0.58	0.66
EU+US	0.60	0.63	0.62	0.65
$(EU+US)_{EU}$	0.62	0.67	0.63	0.70
$(EU+US)_{US}$	0.59	0.61	0.58	0.62

**Table 2:** DFA-2 scalings in each subsystem, for each of the measured quantities. Symbols as in Table 1.

**Figure 1:** Loglog plots of fluctuation function values versus  $\Delta n$  for  $\rho_A$  (radius of co-assignment) in the 3 selected subsystems (EU, US, EU+US) and in the EU/US subsystems when embedded into the EU+US subsystem. Black solid lines show the linear fit we use to estimate the DFA-2 scaling.



195 radius of co-invention, showing a perhaps greater ease of establishing stable connections,  
 196 even at longer distance, within the US subsystem. It has to be noted that this might also  
 197 stem, for instance, from a more geographically sparse distribution of company locations.  
 198 This last hypothesis might also explain the discrepancy between the co-assignment and  
 199 the higher co-invention scaling values for the US subsystem.

200 To single out the contribution of “leading nodes”, i.e. the nodes showing a significant  
 201 monotonic trend (see Table 1), we estimate the scaling when all these nodes are removed  
 202 from each subsystem. Table 3 shows the results of this analysis. Scaling values become  
 203 generally closer to the “uncorrelated” mark ( $\alpha = 0.5$ , which would entail that the un-  
 204 derlying signal can be associated to white noise and, as such, nothing can be said about  
 205 its persistence in time), but, still, they lie outside the 95<sup>th</sup> percentile threshold values  
 206 for uncorrelated signals. In general, subsystems do not seem to change their qualitative  
 207 behavior and can be said to be robust to the removal of their most performing nodes. It  
 208 stems from these results that the increasing patterns that are observed in technological  
 209 collaboration metrics at continental level can be considered persistent in time, regardless  
 210 of the underlying trend and of the presence of the most performing nodes.

## 211 4.1 Long-term correlation at EU national level

212 Results, so far, show a general picture that looks remarkably similar, at least qualitatively,  
 213 for all metrics and subsystems we have taken into account. The structure of the data

Subsystem	$\rho_A$	$\rho_I$	$CB_A$	$CB_I$
EU	0.61	0.63	0.59	0.58
US	0.58	0.60	0.57	0.61
EU+US	0.59	0.60	0.59	0.58
$(EU+US)_{EU}$	0.61	0.62	0.60	0.58
$(EU+US)_{US}$	0.57	0.60	0.57	0.58

**Table 3:** DFA-2 scaling values in each subsystem, for each of the measured quantities, when nodes showing monotonic trends (see Table 1) are removed. Symbols as in Table 1.

214 allows us, though, to perform a much more particular analysis, i.e. at EU national level.  
215 In this context, we point out that several political initiatives are currently in place to  
216 favor the integration of the European R &D collaboration system (see e.g. Schengell and  
217 Lata, 2013; Chessa et al., 2013; Arrieta et al., 2017).

218 To see whether reducing the geographical scale of the analysis might unravel differ-  
219 ent properties of local systems and, thus, relevant heterogeneities within the EU system,  
220 we single out 18 EU countries having more than 10 “active” regions in at least one of  
221 the datasets (i.e. they have at least 10 regions having at least one co-assignment or  
222 co-invention in the selected time span), and estimate their correspondent DFA-2 scaling  
223 for all metrics. Table 4 shows the list of selected countries and the results of this anal-  
224 ysis. We include “partial” or younger EU members to see whether longer or fuller EU  
225 membership is associated with DFA-2 scaling results. We remark here that, due to the  
226 lower number of data points at national scale, we treat as potentially uncorrelated all  
227 scaling values below a 95<sup>th</sup> percentile threshold (marked with a star in Table 4), that we  
228 obtain from generating uncorrelated synthetic signals (see the Appendix for details). In  
229 this respect, although there is not enough information to perform a thorough statistical  
230 analysis, it seems notable that uncorrelated behavior can arise both “within” (as in the  
231 Portugal case) and outside EU-15 borders, and viceversa (see e.g. Hungary and Poland,  
232 where relationships between inventors, especially, seem to be maintained in time, whereas  
233 it seems much more unlikely for Polish and Hungarian companies to participate in a  
234 co-assignment). Switzerland emerges as the best performing country for all metrics, pin-  
235 pointing the role of geographical (i.e. the country being a natural continental hub in this  
236 respect, not to mention the compresence of several languages) but also institutional (i.e.  
237 the high number of multinational corporation HQs and of international organizations)  
238 factors in maintaining long-distance collaborations in time.

239 Moreover, it also seems relevant to investigate which countries improve their scaling  
240 when US nodes are taken into account while calculating the selected metrics. Figure  
241 2 shows the results (in terms of percentage change) for all countries and metrics. We  
242 single out variations exceeding the average estimation error for the relative number of  
243 active regions in each country and for each metric (see the Appendix for details). Also,  
244 we highlight increments/decrements that bring the scaling above/below the uncorrelation  
245 threshold we have set for that country and metric (see Table A1 in the Appendix). We  
246 group countries in positively, negatively and contrasted/neutrally affected groups, based  
247 on the presence of a significant increase, or decrease, or no significant change/concurrent  
248 presence of significant decrease and increase, respectively. Interestingly, this grouping  
249 highlights relatively coherent blocks, in terms of economic relationships. As expected, this  
250 analysis pinpoints the national systems which have stronger relationships, traditionally,



Country	$\rho_A$	$\rho_I$	$CB_A$	$CB_I$
Austria: AT	0.68	0.72	0.68	0.78
Belgium: BE	0.62	0.71	0.69	0.78
Bulgaria: BG	0.52*	0.58*	0.57*	0.67
Switzerland: CH	0.77	0.81	0.86	0.92
Germany: DE	0.63	0.70	0.63	0.70
Greece: EL	0.60*	0.60*	0.52*	0.53*
Spain: ES	0.65	0.68	0.61	0.66
France: FR	0.61	0.70	0.65	0.78
Croatia: HR	0.56*	0.61*	0.62*	0.51*
Hungary: HU	0.60*	0.73	0.51*	0.74
Italy: IT	0.65	0.70	0.62	0.68
Netherlands:NL	0.60	0.68	0.65	0.78
Poland: PL	0.52*	0.73	0.54*	0.66
Portugal: PT	0.48*	0.66	0.45*	0.60*
Romania: RO	0.51*	0.61	0.51*	0.55*
Sweden: SE	0.62	0.76	0.53*	0.78
Turkey: TR	0.48*	0.55*	0.46*	0.56*
United Kingdom: UK	0.61	0.59	0.63	0.69

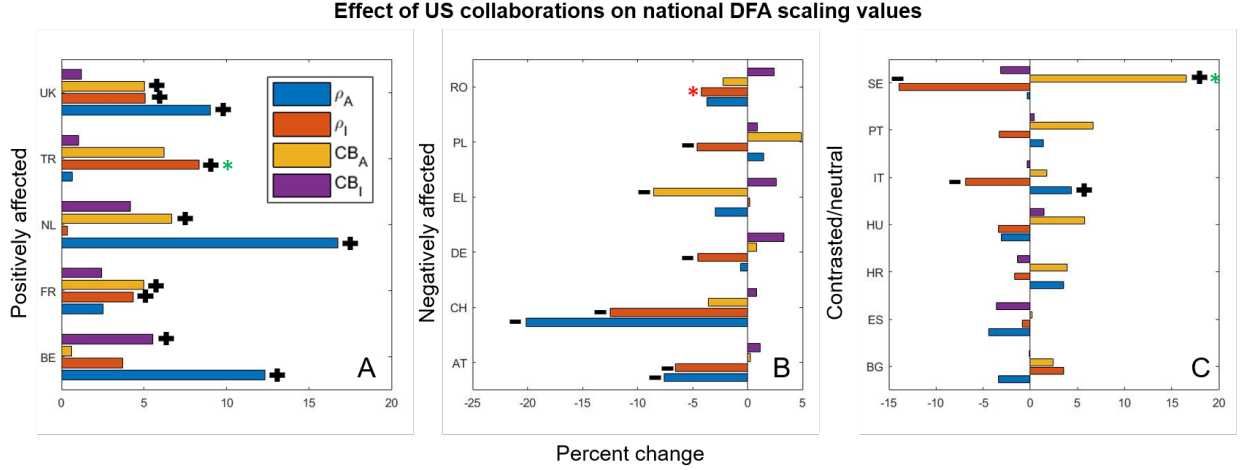
**Table 4:** DFA-2 scaling values in each of the selected 18 EU countries, when only EU nodes are taken into account, for all measured quantities. Symbols as in Table 1. All country codes refer to the ISO classification, except for Greece (EL). '\*': values below the 95<sup>th</sup> percentile threshold for uncorrelated signals listed in Table A1 in the Appendix.

251 with the US, such as the UK and Turkey. The significant increase in the DFA metrics  
252 of these countries, that is observed when US collaborations are accounted for, implies  
253 that the collaborations with US firms and inventors are long-standing and persistent in  
254 time. In particular, when you remove US collaborations, the time series for the radius  
255 of co-invention in Turkey become uncorrelated in time, even. Interestingly, also countries  
256 which entertain solid relationships with the UK display a steady increase in all metrics (i.e.  
257 Belgium, Netherlands and France; see panel A in Fig.2). On the contrary, the grouping of  
258 negatively affected countries reveals a block of notoriously interconnected countries from  
259 the economic point of view (i.e. Austria, Germany, Switzerland, Poland and Romania).  
260 Interestingly, Switzerland emerges as the most negatively affected country, as only the  
261 scaling of cross-border co-invention links increases, rather slightly. We note that this  
262 does not imply necessarily that Switzerland is performing worse than other countries (e.g.  
263 has less collaborations with the US; as hinted by data on life sciences industry in [Owen-](#)  
264 [Smith et al., 2002](#), the opposite is probably true), but that its collaborations with the US  
265 are more erratic, which also means that they could be more ubiquitous and dynamic. All  
266 other countries show a non-univocal behavior, although many improve their co-assignment  
267 scaling value, and, more expectedly, cross-border links become more stable in time.

## 268 4.2 Correlation of national DFA scaling values with features of 269 the local collaboration graph

270 From the previous results, it seems apparent that external factors play a role in deter-  
271 mining the observed scaling values in different countries. Correlations between patenting

**Figure 2:** Percentage changes in DFA-2 scalings for all the selected metrics and in each of the selected EU countries, when the whole EU+US subsystem is considered in metrics calculation. Positive values indicate that metrics increase when US collaborations are accounted for, and viceversa. Light blue bars: radius of co-assignment  $\rho_A$ ; dark orange: radius of co-invention  $\rho_I$ ; yellow: cross-border links in co-assignments  $CB_A$ ; purple: cross-border links in co-inventions  $CB_I$ . '+/-': the positive/negative difference is higher in magnitude than the average estimation error for the corresponding length of the time series (see the Appendix and Table A1). '\*': the difference is such that the scaling passes from uncorrelated to correlated (green star) or viceversa (red star). Uncorrelation is defined according to the thresholds in Table A1 in the Appendix. Panel A (“Positively affected”): countries whose metrics are positively affected by US collaborations (i.e. at least one shows a significant increase and, concurrently, there are no significant decreases). Panel B (“Negatively affected”): countries whose metrics are negatively affected by US collaborations (i.e. at least one shows a significant decrease and, concurrently, there are no significant increases); Panel C (“Contrasted/neutral”): countries whose metrics show either no significant change, or concurring significant increases and decreases.



272 rates in general and local economies have been studied in the past (Guellec and de la  
273 Potterie, 2001; De Rassenfosse and van Pottelsberghe de la Potterie, 2007) and seem  
274 redundant in our case. What might be more interesting, perhaps, is to see whether cer-  
275 tain features of the national collaboration networks can be associated with the observed  
276 scaling values. This might shed light on the organizational properties of national R&D  
277 systems that seemingly promote a greater persistence of technological collaboration time  
278 series. In this context, we point out that our previous results on the heterogeneity of DFA  
279 scaling values among EU countries and, also, of their dependence on US collaborations,  
280 show that a completely integrated European Research Area is far from being fulfilled.  
281 This is interesting also from a policy perspective, since it is known that, for instance,  
282 EU initiatives towards technological collaboration have been directed to increase certain  
283 properties of the EU R&D network (e.g. clustering), even though the impact on actual  
284 knowledge diffusion is controversial (Cowan and Jonard, 2004). To this end, we extract  
285 the cumulative weighted adjacency matrices of the selected countries for years 2010-2014,  
286 in which the weight of each link is defined as the inverse of the number of collaborations  
287 between each pair of nodes. We use this cumulative network as a representation of the  
288 current state of the collaboration network, in terms of topological properties. This is  
289 performed for co-assignment and co-invention networks both. We then calculate a set of  
290 graph properties that we deem relevant to describe the topological structure of the net-  
291 work (i.e. density, assortativity, average closeness, network clustering coefficient, central  
292 point dominance and diameter). We then correlate these topological features with the  
293 observed scaling values, normalized by the corresponding standard deviation to account  
294 for the different variances arising from different numbers of active regions and different

295 scaling values (see the Appendix for details). Results are shown in Table 5.

296 In general, only co-assignment scaling values turn out to exhibit significant correla-  
 297 tions with graph properties, hinting at the fact that systemic properties might be more  
 298 important for co-assignment time series, rather than for co-invention ones. This was  
 299 also apparent from the actual scaling values (Table 5), where countries with seemingly  
 300 uncorrelated co-assignment time series had positively correlated co-invention time series.

301 Among all the graph properties we extracted, a few ones emerge as associated with  
 302 higher DFA scaling values. In particular, the diameter (i.e. the greatest distance between  
 303 any pair of vertices) of national co-assignment networks is positively correlated to DFA  
 304 scaling values at very high significance level, highlighting the role of more developed  
 305 and complete networks. Assortativity (a measure of the attachment preference to nodes  
 306 with similar degree) and clustering are the other two important characteristics showing  
 307 significant, positive correlations with DFA scaling values. Considering that all these three  
 308 features show themselves significant, positive cross-correlations, it results that persistence  
 309 in time of the co-assignment metrics is related to systems with specialized – but strongly  
 310 connected – subnational clusters.

Graph metric	$\rho_A$	$\rho_{A,US}$	$CB_A$	$CB_{A,US}$	$\rho_I$	$\rho_{I,US}$	$CB_I$	$CB_{I,US}$
Density	0.14	0.16	0.03	0.03	0.35	0.32	0.43	0.43
Assortativity	0.49*	0.50*	0.55*	0.55*	-0.05	-0.06	0.04	0.04
Closeness	0.24	0.22	0.33	0.32	0.03	0.01	-0.01	0.01
Clustering	0.44	0.43	0.51*	0.49*	0.29	0.28	0.23	0.23
CPD	0.27	0.26	0.23	0.21	-0.11	-0.11	-0.22	-0.23
Diameter	0.71**	0.71**	0.71**	0.71**	-0.14	-0.16	-0.03	-0.03

**Table 5:** Correlation coefficients between normalized DFA-2 scalings in each of the selected 17 EU countries and the corresponding graph metrics (CPD: Central Point Dominance). Asterisks show the p-value associated with the statistically significant correlation coefficients: \*:  $p < 0.1$ ; \*\*:  $p < 0.05$ . Other symbols as in Table 1.

## 311 5 Conclusions

312 We have applied Detrended Fluctuation Analysis to time series of selected metrics con-  
 313 cerning international patent collaborations (be them co-assignments or co-inventions),  
 314 based on the OECD RegPat database. In particular, we have focused on two metrics:  
 315 the average yearly radius of collaboration and the yearly number of cross-border collabo-  
 316 rations. We have extracted these metrics at the level of OECD TL3 regions, the spatial  
 317 segmentation provided by RegPat, limited to the EU and US systems.

318 We can summarize the main conclusions of this work as follows:

- 319 • when evaluating long-term correlation properties at “continental” scale (that is, EU,  
 320 or US, or EU+US), the time series of the selected metrics show that the increases  
 321 that we observe in our data set are persistent in time and, as such, can be expected to  
 322 protract after our observation period; also, these persistence properties are resistant,  
 323 to some extent, to the removal of the best performing regions;
- 324 • when calculating scaling values at EU national level, different qualitative and quan-  
 325 titative behaviors emerge; the observed changes in scaling values when US collabo-  
 326 rations are taken into account shed light on which countries have stronger overseas

relationships; in particular, the UK, Turkey and traditionally related countries such as Belgium, France and the Netherlands all increase their persistence metrics, when US collaborations are accounted for; on the contrary, the “German block” (i.e. Germany and German-speaking countries and also German neighbors such as Poland) shows significant decreases;

- even though the number of selected nations is necessarily low, several and significant associations between DFA scaling values and features of the national internal collaboration graph are found; in particular, co-assignment persistence in general emerges as correlated to the diameter (i.e. the maximum distance in the graph), assortativity (i.e. the attachment preference of nodes to nodes of similar degree) and clustering of said graph, highlighting the role of the development of national R&D systems in guaranteeing persistence of international or simply long-distance collaborations.

We maintain that this study can help deepen our understanding of the intrinsic properties of the evolution of international cooperation on R&D, in terms of the persistence in time of the distance between collaborating regions and of the number of cross-border collaborations each region has. In particular, our results confirm that there is a general, persistent increase of relevant metrics of international technological collaborations, especially in the EU, but they also show that the performance of single EU countries and also the dependence on US collaborations are extremely varied. This latter result can shed further light on the difficulties in creating a fully integrated European Research Area.

Despite the shortcomings of the data (i.e. series being short and, often, non-stationary), we have performed several controls on our estimation of the DFA scaling to improve the consistency of our results. Up to now, applications of DFA to short data series have been scarce, to the best of our knowledge, and we believe that our effort represents a relevant methodological advance in this respect. In particular, with respect to previous literature ([Viswanathan et al., 1996](#)), we have provided a procedure to associate measures of statistical confidence to the observed scaling values.

Having highlighted the limitations of this study, a more extensive characterization of spatial-temporal patterns of international collaboration can come from the study of individual inventors, especially when a finer time scale can be accounted for. Studies on the exploration of the “space of ideas” are also a potential extension of this method to the study of innovation processes. A finer time scale is available from the USPTO open dataset ([US Patent and Trademark Office, 2018](#)), even though such individual-based study has to rely on a thorough disambiguation of patent records. A few methods indeed have been applied with considerable effort and success ([Li et al., 2014](#); [Morrison et al., 2017](#)), so we believe this study might set a new path for time series analysis in the field of innovation studies.

## References

- 365
- 366 Arora, A.; Gambardella, A. *Res Policy* **1994**, *23*, 523–532.
- 367 Arora, A.; Fosfuri, A.; Gambardella, A. *Ind Corp Change* **2001**, *10*, 419–451.
- 368 Orsenigo, L.; Pammolli, F.; ; Riccaboni, M. *Res Pol* **2001**, *30*, 485–508.
- 369 Freeman, C. *Res Policy* **1991**, *20*, 499–514.
- 370 Chessa, A.; Morescalchi, A.; Pammolli, F.; Penner, O.; Petersen, A. M.; Riccaboni, M.  
371 *Science* **2013**, *339*, 650–651.
- 372 Morescalchi, A.; Pammolli, F.; Penner, O.; Petersen, A. M.; Riccaboni, M. *Res Policy*  
373 **2015**, *44*, 651–668.
- 374 Frenken, K.; Hoekman, J.; Kok, S.; Ponds, R.; van Oort, J., F. and van Vliet In *Death*  
375 *of Distance in Science? A Gravity Approach to Research Collaboration.*; Pyka, A.,  
376 Scharnhorst, A., Eds.
- 377 Hoekman, J.; Frenken, K.; Tijssen, R. *Res Pol* **2010**, *39*, 662–673.
- 378 Waltman, L.; Tijssen, R.; van Eck, N. *J Inform* **2011**, *5*, 574–582.
- 379 Maisonobe, M.; Eckert, D.; Grossetti, M.; Jegou, L.; Milard, B. *J Inform* **2016**, *10*,  
380 1025–1036.
- 381 Peng, C.-K.; Buldyrev, S. V.; Havlin, S.; Simons, M.; Stanley, H. E.; Goldberger, A. L.  
382 *Phys Rev E* **1994**, *49*, 1685.
- 383 Hardstone, R.; Poil, S.-S.; Schiavone, G.; Jansen, R.; Nikulin, V. V.; Mansvelde, H. D.;  
384 Linkenkaer-Hansen, K. *Front Physiol* **2012**, *3*, 450.
- 385 Viswanathan, G. M.; Afanasyev, V.; Buldyrev, S.; Murphy, E.; Prince, P.; Stanley, H. E.  
386 *Nature* **1996**, *381*, 413.
- 387 Disdier, A.-C.; Head, K. *Rev Econ Stat* **2008**, *90*, 37–48.
- 388 Hu, K.; Ivanov, P. C.; Chen, Z.; Carpena, P.; Stanley, H. E. *Phys Rev E* **2001**, *64*, 011114.
- 389 Owen-Smith, J.; Riccaboni, M.; Pammolli, F.; Powell, W. W. *Manag Sci* **2002**, *48*, 24–43.
- 390 Delignieres, D.; Ramdani, S.; Lemoine, L.; Torre, K.; Fortes, M.; Ninot, G. *J Math Psychol*  
391 **2006**, *50*, 525–544.
- 392 Bryce, R.; Sprague, K. *Nat Sci Rep* **2012**, *2*, 315.
- 393 Castillo, R. D.; Kloos, H.; Holden, J. G.; Richardson, M. J. *Front Physiol* **2015**, *6*, 138.
- 394 Schengell, T.; Lata, R. *Pap Reg Sci* **2013**, *92*, 555–577.
- 395 Arrieta, O. A. D.; Pammolli, F.; Petersen, A. *Sci Adv* **2017**, *3*, e1602232.

- 396 Guellec, D.; de la Potterie, B. v. P. *Res Policy* **2001**, *30*, 1253–1266.
- 397 De Rassenfosse, G.; van Pottelsberghe de la Potterie, B. *OxRep* **2007**, *23*, 588–604.
- 398 Cowan, R.; Jonard, N. *JEDC* **2004**, *28*, 1557–1575.
- 399 US Patent and Trademark Office, PatentsView database. 2018; <http://www.patentsview.org/>.
- 400
- 401 Li, G.-C.; Lai, R.; D’Amour, A.; Doolin, D. M.; Sun, Y.; Torvik, V. I.; Yu, A. Z.; Fleming, L. *Res Policy* **2014**, *43*, 941–955.
- 402
- 403 Morrison, G.; Riccaboni, M.; Pammolli, F. *Nat Sci Rep* **2017**, *4*, 170064.

## 404 A Appendix

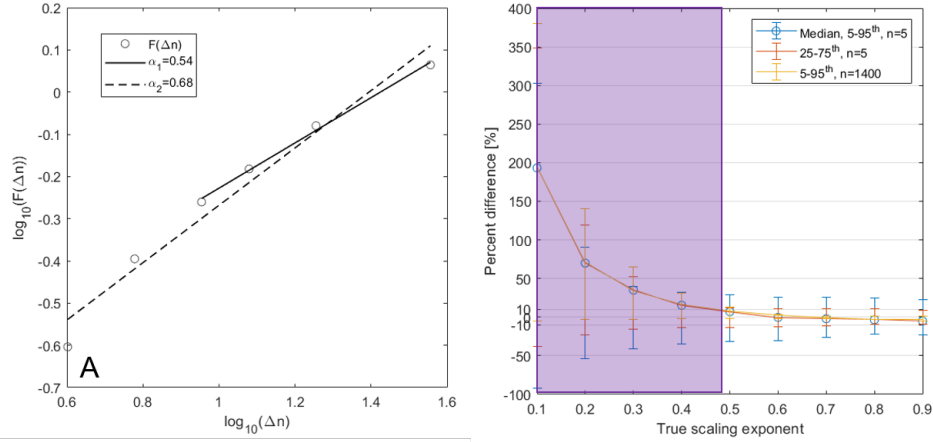
### 405 A.1 Specific methodology of DFA application

406 We devise a specific methodology to recover the DFA scaling value, given the particular  
 407 conditions of our case study, i.e. short, “composite” time series, possibly characterized  
 408 by non-stationarity. We generate  $n$  synthetic Gaussian noise series of length  $t$  (in our  
 409 case,  $t = 36$ ), characterized by a specific scaling value (i.e.  $\alpha = 0.5$ ). Here, we choose  
 410  $n = 1000$  to decrease the estimation error and thus to pinpoint the effects of trend. As  
 411 performed in [Hu et al. \(2001\)](#), we superimpose to an arbitrary fraction of these series  
 412 a trend of a given order. We estimate the DFA scaling for 1,000 realizations and for  
 413 different values of the fraction of nodes with a superimposed trend (spanning from 10%  
 414 to 100%). In general, we note that DFA can best detect the true scaling of the underlying  
 415 signal when the first two window lengths (i.e.  $\Delta n = \{4, 6\}$ ), which likely suffer from bad  
 416 parameterization, are discarded (Fig. A.1A). In the DFA-1 case, scaling turns out to be  
 417  $\simeq 2$  as in [Hu et al. \(2001\)](#) for any non-negative fraction of nodes with a linear trend  
 418 ( $\alpha_{DFA-1} = 2.00 \pm 6.34 \cdot 10^{-4}$ ). The distributions of estimated DFA scalings at different  
 419 values of the fraction of nodes with a trend, instead, turn out to be indistinguishable  
 420 from the one coming from realizations with no trend superimposition in a two-sided  
 421 Wilcoxon rank-sum test ( $\alpha_{DFA-2} = 0.54 \pm 1.5 \cdot 10^{-3}$ ; see below for a quantitative analysis  
 422 of the estimation error). At the same time, the presence of higher order trends (e.g.  
 423 quadratic) in a fraction of the  $n$  series would manifest in a clearly non-stationary scaling  
 424 (i.e.  $\alpha_{DFA-2} = 3.05 \pm 3.16 \cdot 10^{-4}$ ). Thus we make use of DFA-2 as the best trade-  
 425 off between detrending power and local overparameterization (our window lengths being  
 426 highly constrained at  $t = 36$ ).

### 427 A.2 Additional controls

428 We find appropriate, due to the low absolute number of data points and to the shortness of  
 429 the maximum window length, to assess quantitatively the degree of error associated with  
 430 our estimate, as revealed e.g. by Fig. A.1A. To this end, we perform 1,000 repetitions  
 431 of the synthetic series generation, at varying scaling values, and calculate the average  
 432 error between our estimate and the true scaling. For comparison purposes, we repeat

**Figure A.1:** Panel A: loglog plot of fluctuation function values versus the corresponding window length of 1,400 synthetically generated time series of total length 36 (gray circles) and fixed scaling (0.5). The black solid line shows the linear fit over the last 4 window lengths, while the dashed solid line shows the linear fit over the whole set of window lengths. Panel B: average and error bars between estimated and true DFA-2 scaling for 1,000 repetitions of time series generation, at varying scaling and number of nodes  $n$ . Light blue circles show the median error, while whiskers extend to distribution percentiles (light blue: 5-95<sup>th</sup>,  $n = 5$ ; dark orange: 25-75<sup>th</sup>,  $n = 5$ ; yellow: 5-95<sup>th</sup>,  $n = 1400$ ). The lilac shaded panel excludes the scaling values that are outside the range found in this paper’s results.



433 this simulation for the aforementioned minimum value  $n = 5$  and for  $n = 1400$ , which is  
 434 approximately the number of “active” EU regions (i.e. appearing in the RegPat database)  
 435 and, thus, represents a measure of the value of  $n$  we use at the aggregate scale. We show  
 436 in Fig. A.1B that this error converges to zero for growing values of the true underlying  
 437 scaling. When  $n = 5$ , only in a few cases the error goes beyond 10%, for extreme values  
 438 of the 5-95<sup>th</sup> error bar. Increasing the number of nodes does not change the median error  
 439 dramatically but narrows the distribution of error values considerably. This seems in  
 440 accordance with similar results on short data series shown in [Delignieres et al. \(2006\)](#).  
 441 Much greater deviations are found when the underlying series is anti-correlated (shaded  
 442 area in Fig. A.1B), but we anticipate that this is almost never found in our results.

443 Due to the relatively high standard deviation that is found when the number of regions  
 444 under study is low, we deem necessary to have a measure of confidence when discriminating  
 445 between uncorrelated and long-term correlated signals. This is particularly relevant for  
 446 the national scale analysis, when the number of active regions spans from 5 to 402. To  
 447 this end, we retrieve the 95<sup>th</sup> percentile value of the scaling value observed in, again,  
 448 1,000 repetitions of synthetic series generation of an uncorrelated signal ( $\alpha = 0.5$ ), for  
 449 each value of the number of regions that we find in the selected countries (see Table  
 450 A1 for the complete list). This corresponds to performing a 1-tailed t-test and sets  
 451 a sort of threshold above which we exclude uncorrelation in the observed data, with  
 452 relative safety. Additionally, we compute the average percent error from the true scaling  
 453 to have a comparison value for the variations we observe i.e. when considering EU/US  
 454 collaborations at national scale. Table A1 shows both threshold values for all the values  
 455 of the number of active regions and their correspondent country. We do not report results  
 456 regarding the super-national scale, as our results are all well beyond the threshold value  
 457 in all these cases.

458 We also deem necessary to account for the different standard deviations we observe  
 459 when varying number of active regions, especially when we correlate the observed scalings

460 to exogenous factors (see Section 4). To this end, we normalize the observed scalings  
461 by their associated standard deviation, which we obtain by observing the distribution of  
462 1,000 synthetic realizations of signals having the same parameters (i.e. DFA true scaling,  
463 number of active regions). This is meant to remove the confounding effect of different  
464 variances in the data, when performing correlation analysis.

Country	$n_{\rho_A}$	$\alpha_{95}$	$\Delta\%$	$n_{\rho_I}$	$\alpha_{95}$	$\Delta\%$	$n_{CB_A}$	$\alpha_{95}$	$\Delta\%$	$n_{CB_I}$	$\alpha_{95}$	$\Delta\%$
AT	33	0.59	5.8	35	0.59	5.7	33	0.59	5.8	35	0.59	5.7
BE	44	0.59	5.3	44	0.59	5.3	38	0.59	5.5	44	0.59	5.3
BG	10	0.64	9.6	23	0.61	6.7	5	0.68	13.2	14	0.63	8.3
CH	26	0.60	6.4	26	0.60	6.4	25	0.61	6.6	26	0.60	6.4
DE	401	0.55	3.4	402	0.55	3.4	333	0.56	3.5	402	0.55	3.4
EL	29	0.60	6.1	39 <sup>1</sup>	0.59	5.4	25	0.61	6.6	33	0.59	5.8
ES	50	0.58	5.0	56	0.58	4.9	41	0.59	5.5	54	0.58	5.0
FR	95	0.57	4.3	96	0.57	4.3	87	0.57	4.4	96	0.57	4.3
HR	11	0.64	9.2	19	0.61	7.1	7	0.67	11.3	15	0.62	8.0
HU	20	0.61	7.0	20	0.61	7.0	13	0.63	8.5	20	0.61	7.0
IT	109	0.57	4.1	110	0.57	4.0	80	0.57	4.5	107	0.57	4.1
NL	40	0.59	5.5	40	0.59	5.5	39	0.59	5.4	40	0.59	5.5
PL	55 <sup>2</sup>	0.58	5.0	72	0.58	4.5	26	0.60	6.4	69	0.58	4.6
PT	19	0.61	7.1	23	0.61	6.7	11	0.64	9.2	20	0.61	7.0
RO	13 <sup>3</sup>	0.63	8.5	36	0.59	5.7	8	0.65	10.6	30	0.60	6.2
SE	21	0.61	6.9	21	0.61	6.9	21	0.61	6.9	21	0.61	6.9
TR	27	0.60	6.2	50	0.58	5.0	9	0.65	9.9	31	0.60	6.1
UK	120 <sup>4</sup>	0.57	4.0	125	0.57	3.9	101	0.57	4.2	124	0.57	4.1

**Table A1:** Number of active regions in each country and for each measured metric ( $n_{\rho_{A/I}}$ ,  $n_{CB_{A/I}}$ ) together with corresponding control statistics.  $\alpha_{95}$  represents the 95<sup>th</sup> percentile value of the distribution of the estimated scalings in 1,000 repetitions of a synthetically generated series with true  $\alpha = 0.5$ .  $\Delta\%$  is the percent error between the estimated and the observed scalings, averaged along the 1,000 repetitions of different values of the true scaling, ranging from 0.5 to 0.9, is also shown. Other symbols as in Table 1. Superscripts in the number of active regions indicate a difference between the EU-only and the EU+US cases. <sup>1</sup>:  $n = 40$ ,  $\alpha_{95} = 0.59$ ,  $\Delta\% = 5.5$ ; <sup>2</sup>:  $n = 56$ ,  $\alpha_{95} = 0.58$ ,  $\Delta\% = 4.9$ ; <sup>3</sup>:  $n = 14$ ,  $\alpha_{95} = 0.63$ ,  $\Delta\% = 8.3$ ; <sup>4</sup>:  $n = 121$ ,  $\alpha_{95} = 0.57$ ,  $\Delta\% = 4.1$ .